## PAPER

Check for updates

# Impact of hydrolysis pretreatment on the compostability of biodegradable poly(caprolactone) and poly(lactic acid) films†

Jordan D'Amario,[a] Wanwarang Limsukon,[a,b] Anibal Bher*[a] and Rafael Auras [ID] *[a]

The biodegradation performance of non-pretreated and pretreated commercial polyesters was evaluated under simulated composting conditions to understand how abiotic pretreatment accelerates biotic degradation. Polylactic acid (PLA) and polycaprolactone (PCL) were subjected to hydrolysis pretreatment and assessed under simulated composting conditions for 120 days. In addition to tracking $CO_2$ evolution, polymer-intrinsic factors such as chain scission, measured by reductions in intrinsic viscosity molecular weight ($M_\eta$), and changes in crystallinity ($X_c$) were also evaluated for both non-pretreated and pretreated samples during the biodegradation process. Hydrolysis pretreatment resulted in a reduction of initial $M_\eta$ and an increase of initial $X_c$ for all polymer samples. The initial decrease in $M_\eta$ was particularly marked for PLA, which showed about 30% decrease, while PCL exhibited a reduction of just around 7%. Regarding initial $X_c$, the most significant increase was also seen in PLA, which jumped from approximately 0% to c. 30%. Hydrolysis of semi-crystalline polymers primarily affects the amorphous region, where elevated temperatures allow water to break polymer chains easily. However, for PLA, the disruption of the crystalline structure leads to a less stable type of crystal, probably due to an increase in the rigid amorphous region that enhances the overall biodegradation process. The effect of pretreatment on the biotic phase showed minimal differences for PCL but a noticeable overall increase in biodegradation for the pretreated PLA.

## 1. Introduction

Recent legislative developments in biotechnology and biomanufacturing highlight the need for increased bio-based and recyclable-by-design polymers capable of replacing over 90% of current plastics and commercial polymers at scale by 2030.[1] Initially, this initiative only partially considered managing biodegradable materials due to their lower production levels than traditional non-biodegradable polymers. However, industries have been shifting towards replacing single-use plastics with reusable, recyclable, and even industrial and home-compostable options to foster sustainable practices. Nonetheless, recycling infrastructure has struggled to meet ambitious corporate recycling goals, as approximately 25 to 47% of collected materials are lost in today's recycling processes, underscoring the necessity to enhance product recyclability and improve recycling rates.[2] Organic waste currently comprises approximately one-third of municipal solid waste globally.[3] Implementing compostable plastics could provide a viable and environmental solution to reduce plastic waste accumulation in the environment while also decreasing the amount of plastic waste sent to landfills and incinerators.[4] Moreover, biodegradable and compostable materials could significantly enhance the end-of-life (EoL) management of organic waste, especially in cases of food-contaminated packaging—such as packaging for meat, microwaveable frozen foods, and soft cheeses—which typically cannot be recycled due to contamination.[5] Instead, these materials could effectively be diverted to composting facilities. Current research, market trends, and consumer preferences collectively indicate a growing demand for sustainable, biodegradable alternatives, particularly for single-use packaging applications.

The transition to biodegradable polymers is a critical step in reducing plastic waste; however, challenges persist in ensuring effective degradation and in avoiding unintended environmental consequences, such as microplastic formation. Microplastics, commonly found in paint, tires, pellets, and personal care items, pose significant environmental risks. Microplastic emissions are projected to rise from 9 million tonne in 2019 to 16 million tonnes by 2040, and existing measures to prevent their release remain insufficient.[6] The variety of sources generating microplastics from macro plastics

[a]*School of Packaging, Michigan State University, East Lansing, 48824 Michigan, USA. E-mail: aurasraf@msu.edu*

[b]*Department of Food Science and Technology, Faculty of Science and Technology, Rajamangala University of Technology Tawan-ok, Sriracha, Chonburi 20110, Thailand*

†Electronic supplementary information (ESI) available. See DOI: https://doi.org/10.1039/d5lp00041f

poses a threat to current technologies like mechanical recycling, which currently operate with low efficiency in managing collected plastic waste. Microplastics harm the environment and may enter our food and bodies, which could lead to adverse health effects such as inflammation, oxidative stress, immune responses, and genotoxicity.[7] While biodegradable polymers offer a promising solution for reducing chemical pollution, their slow degradation rate may allow intermediate or transitory microplastics to form, which can deteriorate soil quality.[8]

Polylactic acid (PLA) is a biodegradable polymer derived from biobased sources, with applications in the medical field, serving as a component in drug delivery systems, degradable structures, and orthopedic supports. Its versatility also extends to single-use plastics, frequently used in items such as bags, liners, and utensils.[9] The physiochemical characteristics of PLA make it a sustainable alternative to fossil-based polymers like polypropylene, polystyrene, and polyethylene terephthalate, aiding its growing role in packaging and medicine.[10] However, even though PLA is commercially compostable according to ASTM and ISO standards—resulting in lactic acid monomers as the ultimate byproduct—consumers may mistakenly think it can decompose in home composting or landfills, which do not provide the necessary conditions for its breakdown and final assimilation.[11]

Polycaprolactone (PCL), on the other hand, is a synthetic polymer derived from crude oil and is often used as a copolymer with PLA to enhance stability.[12] PCL is also extensively used in medical devices and tissue engineering applications where long-term degradation is desirable.[13] Similar to PLA, PCL has gained popularity not only in the medical sector but also in packaging where, due to its compatibility with other biodegradable polymers and processability, blends and composites are being introduced as novelty options even as an active packaging alternative.[14] It has also been reported that the use of PLA and PLA composite materials can improve other properties, such as mechanical and barrier properties, without diminishing their biodegradation performance. In this sense, PLA and PLA reactive blended with thermoplastic starch, both reinforced with graphene nanoplatelets, have been reported to exhibit improved properties and good biodegradability.[15] More recently, PLA has been reinforced with wood fiber,[16] and also reported as a coating for improving barrier properties of kraft paper performing well under composting conditions at the EoL.[17]

Structural modifications can be implemented to accelerate its biodegradation rate, providing a sustainable alternative to single-use plastics.

PCL and PLA, both polymers, are capped with a carboxylic acid terminal group. When examining the effect of hydrolysis on PLA in an aqueous solution, a self-catalytic hydrolysis reaction is observed, which is not seen with PCL.[12] Consequently, the hydrolysis kinetics differ between PCL and PLA, as PLA undergoes a self-catalyzed reaction. Additionally, PCL's faster crystallization rate compared to PLA results in greater crystallinity in the materials observed after degradation. Furthermore,

the hydrolytic degradation of PLA and PCL involves chain scission of the ester bonds upon exposure to water molecules, leading to the fragmentation of the long chains.[18,19]

Biodegradable polymers, such as PLA, encounter challenges in industrial composting systems despite being certified as industrially compostable. Industrial composters often hesitate to accept compostable polymers like PLA because distinguishing them from conventional plastics is difficult, and they can be challenging to fully degrade if industrial operations do not align with laboratory testing.[20] Furthermore, some states impose strict regulations that limit compost contamination to less than 1% weight content of plastic, glass, and metal, making it more difficult to include biodegradable plastics in the composting process.[5] While biodegradable materials present potential solutions, it is crucial to carefully consider their degradation rates and manage them in composting systems to avoid the formation of microplastics.[21] Additionally, PLA's commercial compostability is limited outside of industrial settings due to the thermophilic biotic degradation temperature requirement. PCL's hydrophobic, semi-crystalline structure makes it resistant to environmental degradation, creating further challenges if PLA and PCL are not fully biodegraded by the end of the composting operation.[22]

Methods to accelerate the degradation of biodegradable polymers have been previously summarized and critically analyzed, considering both abiotic and biotic approaches.[22] Abiotic methods involve altering polymer properties during processing or before degradation, while biotic methods rely on microbial activity. Key properties influencing biodegradation include molecular weight ($M_n$), crystallinity ($X_c$), polymer thickness, and surface properties. Abiotic techniques to enhance degradation include UV irradiation, thermal treatments, and chemical modifications that render the polymer more susceptible to microbial activity. For instance, ultraviolet light can induce chain scission, increasing the material's vulnerability to further breakdown; however, it can also induce cross-linking in certain polymers, which can reduce biodegradation.[23,24] Thermal treatments, typically conducted between 70 and 150 °C, help soften the polymer and may increase amorphous regions. However, this method can be challenging to implement since it can also rearrange chains and increase, to some extent, crystallinity.[4] Acid or alkaline treatments, combined with anaerobic digestion, have also proven successful in boosting biodegradation by creating conditions that facilitate faster microbial colonization. However, these methods can be expensive and pose safety risks.[25]

Blending PLA with hydrophilic natural polymers, such as thermoplastic starch, is another method that has shown promise in increasing water vapor permeability and providing a source of microbial nutrients, further enhancing biodegradation.[26] Similarly, studies indicate that incorporating cow dung or other organic fillers into PLA and PCL composites accelerates breakdown in soil, suggesting that strategic blending can be a viable approach to enhancing biodegradability.[27]

Hydrolysis emerges as an effective and practical pretreatment method that addresses many of the challenges other pre-

treatment techniques present. It can break down the amorphous regions of a polymer to increase the number of available sites for enzymatic attack, the biotic step initiated by microorganisms.[22] Hydrolysis also applies to real-life scenarios, as polymers like PLA and PCL naturally undergo hydrolysis when exposed to moisture, leading to gradual degradation over time. However, specific temperature conditions are crucial for gaining meaningful insights into the hydrolysis process.[19] While previous studies have utilized enzymatic hydrolysis, some have struggled to determine whether the weight loss of the polymer resulted from complete biodegradation or from the hydrolytic breakdown of chains into low-molar-mass segments.[26] This highlights the need for research that measures $M_\eta$ both after hydrolysis pretreatment and during biodegradation to assess where weight loss occurs accurately. Hydrolysis is less expensive than other pretreatment methods and offers easy accessibility regarding the necessary components.[22]

Since hydrolysis primarily affects the amorphous regions of each polymer, a hydrolysis pretreatment is likely to have a more significant impact on PLA than on PCL regarding final biodegradation. Therefore, PLA and PCL are ideal candidates for comparing how hydrolysis pretreatment influences their $M_\eta$ and $X_c$, directly affecting their biodegradation rates. Their distinct physiochemical properties and similar applications in biodegradable polymers make them particularly suitable for this comparison. PLA is recognized for its high rate of hydrolyzed degradation due to its autocatalytic properties, establishing it as a common benchmark in biodegradation studies alongside other biodegradable polymers.[12,28] Meanwhile, PCL is a preferred biodegradable polymer because of its versatile mechanical properties and the capacity to adjust degradation kinetics by varying factors such as $X_c$, $M_\eta$, and structural porosity (*e.g.*, porosity and thickness).[18]

This work aimed to evaluate the biodegradation performance under composting conditions of two aliphatic biodegradable polyesters, biobased PLA and fossil-based PCL, both pretreated by hydrolysis. In addition to tracking $CO_2$ evolution, polymer-intrinsic factors such as chain scission, measured by $M_\eta$ reduction, and $X_c$ evolution were also assessed for both non-pretreated and pretreated samples during the biodegradation process.

## 2.  Materials and methods

Ingeo™ biopolymer 2003D poly (96% L-lactic acid) (PLA) resin was purchased from NatureWorks LLC (Minnetonka, MN, US), with a number ($M_n$) and weight average molecular weight ($M_w$) previously reported in the range of 120–121 kDa and 200–235 kDa, respectively.[29] PCL CAPA 6800D with an $M_w$ reported by the manufacturer of 80 kDa was obtained from Ingevity® (North Charleston, SC, US). Cellulose powder (particle size *c.* 20 mm) and chloroform Omnisolv were obtained from Sigma Aldrich (Milwaukee, WI, US).

### 2.1.  Preparation of samples

The PLA and PCL samples were produced using compression molding. Each sheet was made from five grams of either PLA or PCL pellets. Before compressing the PLA or PCL pellets, aluminum foil sheets were preheated for 10 minutes. The PLA pellets sandwiched between two aluminum foils were compressed at 180 °C for three minutes at 33 MPa in a hot press (PHI, City of Industry, CA, US). Meanwhile, the PCL pellets were compressed at 90 °C for three minutes at 33 MPa in the hot press. Immediately after hot pressing, the produced sheets were quenched by storing them in a container with ice dry (*c.* −79 °C) for 10 minutes to prevent recrystallization. After production, all samples were kept at −15 °C until use. The average thickness of the PLA samples was 184 ± 84 μm (7.2 ± 3.3 mil), while the average thickness of the PCL samples was 193 ± 54 μm (7.6 ± 2.1 mil), both determined by averaging ten measurements for each sample using a digital micrometer (Testing Machines Inc., Ronkonkoma, NY, US).

### 2.2.  Pretreatment by hydrolysis

The hydrolysis test was conducted using a batch immersion method in HPLC-grade water under unbuffered conditions. Briefly, PLA and PCL films measuring $1 \times 1$ cm$^2$ were introduced into deionized water at a ratio of approximately 0.62 mL cm$^{-2}$ for PLA and 0.65 mL cm$^{-2}$ for PCL. The hydrolysis conditions for PLA were set at 95 °C for 5 hours, while the PCL samples underwent hydrolysis at 45 °C for 72 hours. After retrieval, the samples were thoroughly dried before further testing and analysis.

### 2.3.  Viscosity-average molecular weight ($M_\eta$) determination

To calculate the $M_\eta$, the Mark–Houwink equation was employed using the intrinsic viscosity ($\eta$) obtained from measurements conducted in accordance with ASTM D2857-16, using chloroform ($CHCl_3$) as the solvent. The intrinsic viscosity was determined using a Rheotek™ RPV-1 (PSL Rheotek, IN, US) automated viscosity measuring instrument, with a Rheotek™ iSP-1 preparation system operating at 30 ± 0.1 °C for PLA and PCL. Each sample was prepared in four different concentrations ranging from 0.125 to 0.500 g dL$^{-1}$. The reduced viscosity and inherent viscosity were plotted against concentration. The intrinsic viscosity value was derived by extrapolating the reduced viscosity and inherent viscosity to zero concentration. The average of the two obtained intercept values was used as the intrinsic viscosity to determine the $M_\eta$ using the Mark–Houwink equation:

$$[\eta] = K \cdot M_\eta^\alpha \tag{1}$$

where $K$ and $\alpha$ are constants, which depend on the nature of the polymer, solvent, and temperature obtained from the intercept and slope of a double logarithmic plot of intrinsic viscosity *versus* $M_\eta$. The $K$ and $\alpha$ values of each material in $CHCl_3$ at 30 °C were obtained from the literature and shown in Table 1.

**Table 1** $K$ and $\alpha$ values for PLA and PCL for the Mark–Houwink equation

| Polymer | Temperature, °C | $K$, $10^{-3}$ mL g$^{-1}$ | $\alpha$ | Ref. |
|---|---|---|---|---|
| PLA | 30 | 0.0131 | 0.777 | 30 |
| PCL | 30 | 0.0130 | 0.828 | 31 |

### 2.4. Crystallinity ($X_c$) measurement

The $X_c$, glass transition temperature ($T_g$), crystallization temperature ($T_c$), and melting temperature ($T_m$) of PLA and PCL were measured using a Differential Scanning Calorimetry (DSC) model Q100 (TA Instruments, New Castle, DE, US) equipped with a mechanical cooling system performed under the heat-only condition with a heating rate of 10 °C min$^{-1}$ from 0 to 180 °C. The degree of $X_c$ was determined using eqn (2) below:

$$X_c = \frac{\Delta H_m - \sum \Delta H_c}{\Delta H_m^\circ} \qquad (2)$$

where $\Delta H_m$ is the enthalpy of fusion from the integration of the heat flow in the melting region, $\sum \Delta H_c$ is the sum of the exothermic enthalpy peaks, and $\Delta H_m^\circ$ is the calculated melting enthalpy of 100% crystalline polymers obtained from the literature. For PCL, this value is 167 J g$^{-1}$ (ref. 32) and for PLA is 93 J g$^{-1}$.[33]

### 2.5. Biodegradation test

PLA and PCL films (8 g) were cut into ~1 cm$^2$ pieces and introduced into a bioreactor (1.9 L) filled with mixed manure-straw compost that had been screened with 10 mm mesh and acquired from the Michigan State University (MSU) Composting Facility (East Lansing, MI, US), along with vermiculite equilibrated with deionized water to enhance the moisture content of the compost (up to 50%) in a 4 : 1 ratio (based on dry weight compost). The measurement of $CO_2$ evolution was conducted for PLA and PCL films in triplicate bioreactors, and the average and standard error values are reported. One additional bioreactor was used for sampling to study $M_\eta$ reduction. Three blank bioreactors (compost without samples) were employed to detect the background $CO_2$ evolution. Three bioreactors with 8 g of cellulose powder were included as a positive control due to cellulose's high biodegradability. The characterization of the compost's physicochemical parameters was conducted by the MSU Soil and Plant Nutrient Laboratory (East Lansing, MI, US), and the results are presented in Table S1 in the ESI.† The biodegradability was evaluated in compost under aerobic conditions using a direct measurement respirometer system, where temperature (58 ± 2 °C), relative humidity (50 ± 5%), and air flow rate (40 ± 2 cm$^3$ min$^{-1}$) were the primary controlled parameters. The methodology and equipment are detailed thoroughly elsewhere.[34] The $CO_2$ evolved from the blank bioreactor was considered the background signal, and this value was subtracted from the amount of $CO_2$ produced by each sample bioreactor to calculate the biodegradation of each sample; where the percentage bio-

degradation represents the total amount of carbon molecules converted to $CO_2$, calculated according to eqn (3) below:

$$\% \text{ of Biodegradation} = \frac{(CO_2)_t - (CO_2)_b}{M_t \times C_t \times \frac{44}{12}} \times 100 \qquad (3)$$

where the numerator is the difference between the average of the three bioreactors' cumulative mass of $CO_2$ evolved for the sample $(CO_2)_t$ and the average $CO_2$ evolved from the three blank bioreactors $(CO_2)_b$. The denominator represents the theoretical amount of $CO_2$ produced by the sample. $M_t$ is the total mass of the sample, $C_t$ is the proportion of carbon present in that sample as determined by CHN analysis, and 44 and 12 are the molecular mass of $CO_2$ and the atomic mass of carbon, respectively.[35] The carbon content for each sample was quantified using a PerkinElmer 2400 Series II CHNS/O Elemental Analyzer (Shelton, CT, US), and results can be found in Table S2 in the ESI.†

## 3. Results and discussion

The leading factors that affect polymer biodegradation are related to the polymer's structure and the environment. Pretreatment focuses on deteriorating the intrinsic polymer structure, such as polymer chain scission (observed by a reduction in $M_\eta$) and crystallinity structure. We have previously reported that abiotic pretreatment of aliphatic polyesters could be reported as a feasible way to enhance overall biodegradation performance, particularly under composting conditions.[22] Targeting the reduction of $M_\eta$ has been one of these methods. In this study, the reduction of $M_\eta$ was achieved through hydrolysis at high temperatures (above the $T_g$ of the samples), and the results of biodegradation performance comparisons between non-pretreated and pretreated samples are discussed.

### 3.1. Effect of abiotic pretreatment on initial molecular weight and initial crystallinity

During hydrolysis pretreatment, water penetrates the entire polymer, causing random hydrolytic chain splits to occur uniformly throughout the matrix. The ester chains are cleaved, forming carboxyl terminal groups that decrease the size of the molecular chains, leading to a reduction in $M_\eta$.[36] Previous studies have shown that $M_\eta$ of polymers declines with increased exposure time in water during hydrolysis.[19] Table 2 displays the $M_\eta$ of PCL and PLA before and after hydrolysis. The $M_\eta$ of PLA-PT is $c.$ 130 kDa, compared to $c.$ 167 kDa for the non-pretreated sample, indicating a 22% reduction. Similarly, for PCL-PT, the $M_\eta$ is $c.$ 93.6 kDa, whereas the $M_\eta$ of the non-pretreated PCL is $c.$ 97 kDa, showing a 3.5% reduction. Apart from crystallinity, the high hydrophobicity of PCL has been recognized as a crucial factor for the slow decrease of $M_\eta$.[37] This underscores the importance of considering surface properties and their alteration through acidity/alkaline treatment to expedite hydrolysis, enzymatic depolymerization, and the overall degradation process in the case of polyesters.[38]

**Table 2** Viscosity-average molecular weight ($M_\eta$), and crystallinity ($X_c$), for PLA, PLA-PT, PCL, and PCL-PT samples before and after hydrolysis. Measured glass transition temperature ($T_g$), and melting temperature ($T_m$) for pretreated and non-pretreated PLA, PLA-PT, PCL, and PCL-PT from DSC before and after hydrolysis

|  | $M_\eta$, kDa | $X_c$, % | $T_g$, °C | $T_m$, °C |
|---|---|---|---|---|
| PLA | 168.8 ± 9.4[a] | 0.4 ± 0.4[a] | 55.4 ± 3.6[a] | 144.2 ± 1.8[a] |
| PLA-PT | 130.3 ± 6.6[b] | 26.8 ± 1.8[b] | 60.3 ± 0.7[a] | 148.8 ± 0.7[a] |
| PCL | 97.0 ± 2.0[a] | 35.1 ± 1.5[a] | — | 51.8 ± 0.4[a] |
| PCL-PT | 93.6 ± 0.8[a] | 42.5 ± 2.7[b] | — | 56.5 ± 0.3[b] |

Within a column and for the same polyester, values followed by a different letter are significantly different at $P \leq 0.05$ (Tukey's test).

The reduction of $M_\eta$ in polymers impacts their $X_c$ fraction in two ways. As $M_\eta$ reduces, chain mobility is enhanced, promoting better alignment and packing of polymer chains; simultaneously, $X_c$ can increase due to chain mobility, so preferentially attacking of the amorphous region occurs. According to the data presented in Table 2, the $X_c$ of amorphous PLA risen from 0% to c. 27% after pretreatment, while the $X_c$ of PCL only increased from c. 35% to c. 43%. In binary blends like PCL and PVC, reduced $M_\eta$ facilitates phase segregation, enabling one polymer to move more freely into interfibrillar regions, promoting crystallization.[32] However, in homogeneous PCL, a large reduction of $M_\eta$ is not observed.

### 3.2. Evolution of PLA, PLA-PT, PCL, and PCL-PT during biodegradation

**3.2.1. Visual inspection.** Fig. 1 illustrates the degradation of PCL (both pretreated and non-pretreated) samples in compost from day 0 to day 18 of the experiment, as PCL samples from day 30 could not be collected. Throughout the 18 day composting period, both non-pretreated and pretreated PCL samples display progressive degradation, characterized by increasing holes, discoloration, and fragmentation. The visual disintegration of samples indicates a correlation between abiotic degradation and $M_\eta$ reduction during the first fifteen days of the test.

Fig. 2 illustrates the degradation of PLA samples (both pretreated and non-pretreated) in compost from day 0 to day 30 of the experiment. The visual disintegration of the samples correlates with abiotic degradation and reduction in $M_\eta$ during the first month of testing. At day 0, a noticeable difference in transparency exists between the samples, particularly between the pretreated and non-pretreated PLA. PLA-PT displays more opaque characteristics than PLA, attributed to the increased $X_c$ developed during hydrolysis, where the crystalline structures are more densely packed.[39] In contrast, PCL shows minimal change in transparency when compared to PCL-PT, as its high initial $X_c$ means hydrolysis has less effect on its appearance than on PLA. A significant difference is noted for PLA pretreated samples when compared to both pretreated and non-pretreated PCL samples, showing a more fragile quality with substantial fragmentation to a powder-like size by day 30, indicative of the characteristic brittle behavior of PLA in contrast to the elastomeric behavior of PCL.

**3.2.2. Evolution of crystallinity and reduction of molecular weight.** Fig. 3 shows the evolution of $X_c$, $M_\eta$ reduction, $CO_2$ evolution, and % biodegradation. The evolution of $X_c$ was measured during the first 30 days of the biodegradation test for both PLA and PCL samples when samples could be collected. Throughout this initial biodegradation period, $X_c$ increased for all samples, with PCL and PCL-PT converging at similar $X_c$ values around day 22, and PLA and PLA-PT approaching similar $X_c$ values around day 28 (Fig. 3a and b).
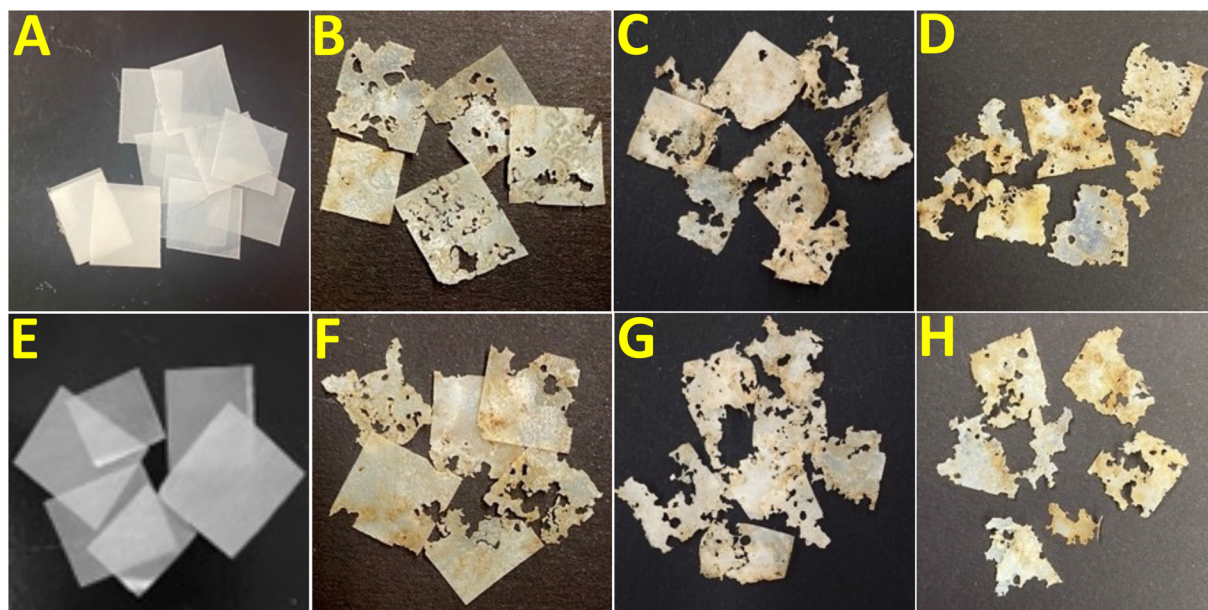


**Fig. 1** PCL non-pretreated day 0 (A), day 6 (B), day 12 (C), day 18 (D) and PCL pretreated day 0 (E), day 6 (F), day 12 (G), day 18 (H) in compost. Note: Initial samples were cut to an area of ~1 cm².
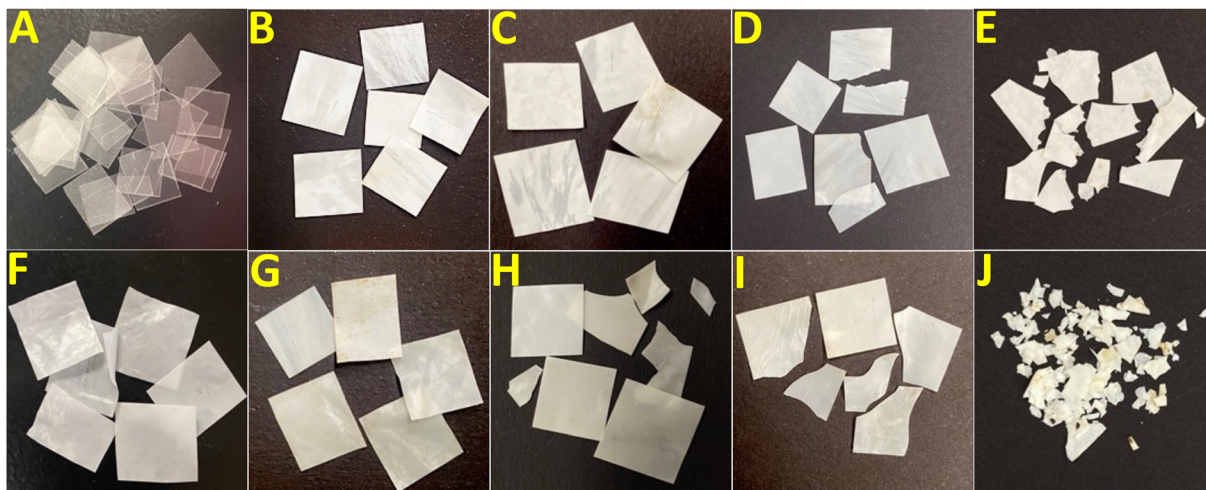
© 2025 The Author(s). Published by the Royal Society of Chemistry

RSC Appl. Polym., 2025, **3**, 711–721 | **715**

**Fig. 2** PLA non-pretreated day 0 (A), day 6 (B), day 12 (C), day 18 (D), day 30 (E) and PLA pretreated day 0 (F), day 6 (G), day 12 (H), day 18 (I), day 30 (J) in compost. Note: Initial samples were cut to an area of ~1 cm$^2$.

Crystallinity increases during biodegradation as hydrolysis primarily breaks down amorphous regions, leaving the more resistant crystalline structures intact. As polymer chains degrade and shorten, they gain mobility, allowing the amorphous regions to reorganize into crystalline structures.[28] Studies on PCL demonstrated that amorphous regions degrade first, leaving behind crystalline material that eventually breaks down. Both PLA and PCL undergo hydrolytic degradation through bulk erosion, where the entire material degrades simultaneously.[39] This selective bulk erosion mechanism of degradation enhances overall crystallinity and slows further degradation, as crystalline regions resist hydrolysis and microbial attack, thereby prolonging material longevity. However, it has been reported that surface erosion patterns, such as grooves and cracks observed in PCL exposed to fungi in compost, further illustrate the persistence and evolution of crystalline structures during biodegradation.[40] Furthermore, Tsuji and Suzuyoshi found that the environmental degradation of PCL can also occur *via* surface erosion rather than bulk erosion, with degradation happening inhomogeneously on the film surface due to microbial attachment.[41] Considering the critical thickness model theory, PCL and PCL-PT samples are deemed to degrade following a bulk erosion mechanism in our test.[39,42] Critical sample thickness for PCL has been reported with a value of *c.* 1.3 cm, indicating a preferred bulk erosion mechanism below that theoretical value.[43] PLA and PLA-PT samples also align with this model, as the critical thickness for poly(α-hydroxy esters) is reported as *c.* 7.4 cm. In this study, the tested samples' thickness remained below this threshold, supporting the conclusion that PLA and PLA-PT samples degraded through a bulk erosion mechanism.[39]

The $M_\eta$ was measured for samples retrieved during the biodegradation test for as long as the samples were available. The values of $M_\eta$ for PLA-PT could not be measured on day 30 using the viscosity technique. In the case of PCL, samples were collected until day 18 of the biodegradation test. Tables S3 and S4 in the ESI† present the $M_\eta$ reduction for PLA and PLA-PT, as well as for PCL and PCL-PT, respectively, while Fig. 3c and d illustrate the normalized $M_\eta$. PLA showed an 86% reduction in $M_\eta$ over the 30 days in compost, while PLA-PT experienced a 70% decrease between day 0 and day 18. For PCL, the $M_\eta$ decreased by 42%, with PCL-PT exhibiting a comparable reduction of 44% during the same 18 day period. The pretreatment performed well for PLA, where a significant portion of the amorphous region was hydrolyzed, achieving destabilization of the three-phase model structure (*i.e.*, crystalline, and rigid and mobile amorphous regions). This allowed for a rapid reduction in $M_\eta$ during the first month of the biodegradation process at a temperature around the $T_g$ of PLA. The high initial $X_c$ influenced the overall decrease in $M_\eta$ for PCL, displaying similar final values before and after pretreatment.

**3.2.3. Evolution of $CO_2$ and biodegradation.** In the case of PLA, the pretreatment resulted in an effective reduction of the abiotic phase by about a week compared to PLA non-pretreated, accelerating the biotic phase. The high rate of PLA-PT biotic phase reached biodegradation of *c.* 100% at day 50, while non-pretreated PLA biodegradation was *c.* 75% at the same point (Fig. 3f and h). In the case of PCL, a small advantage of the pretreatment is observed for PCL-PT, reaching *c.* 100% on day 70, while PCL was *c.* 80% on the same day (Fig. 3e and g). The high initial reduction of $M_\eta$ for PLA (*c.* 22%) played a significant role in reducing the extension of the lag phase and triggering the biotic phase. Furthermore, the increase in initial $X_c$ for PLA by *c.* 30% is indicative that the amorphous phase of PLA structure was highly affected by the hydrolysis pretreatment.

The positive control cellulose reached biodegradation of *c.* 100% at *c.* 40 days. For PLA, abiotic degradation was observed as the controlling mechanism in compost during the first 20 days. A slight acceleration of the abiotic stage was observed for PLA-PT compared to non-pretreated PLA (raw data for biodegradation is provided in Tables S5–S10 in the ESI†).
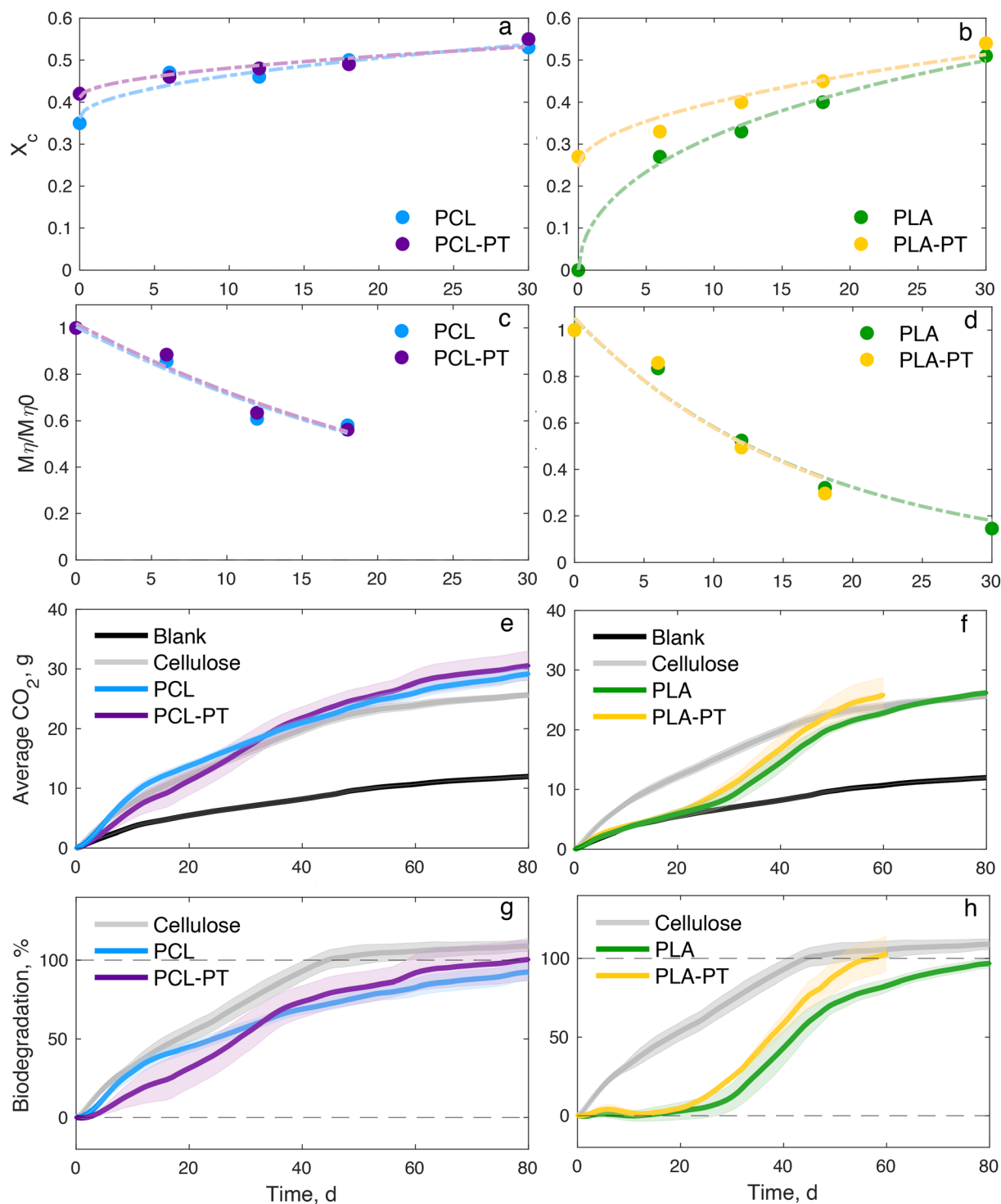
**Fig. 3** (a) crystallinity ($X_c$) evolution of pretreated and non-pretreated PCL, (b) crystallinity ($X_c$) evolution of pretreated and non-pretreated PLA, (c) molecular weight ($M_\eta$) of pretreated and non-pretreated PCL, (d) molecular weight ($M_\eta$) of pretreated and non-pretreated PLA, (e) $CO_2$ evolution of pretreated and non-pretreated PCL, (f) $CO_2$ evolution of pretreated and non-pretreated PLA, (g) biodegradation of pretreated and non-pretreated PCL, (h) biodegradation of pretreated and non-pretreated PLA until day 80. The shade in the background for each material represents the standard error between replicates.

### 3.3. Evolution of thermal properties of samples during biodegradation

Fig. 4 presents the thermal analysis for PCL, PCL-PT, PLA, and PLA-PT samples for day 0 and during the first month of degradation. The $T_g$, $T_c$, and $T_m$ for PCL are reported in the literature as $c.$ −60 °C, 28 °C, and 60 °C, respectively,[44] while PLA typically falls within 50–65 °C for $T_g$, $c.$ 94.5 °C for $T_c$, and 130–180 °C for $T_m$.[45,46] For this work, DSC values measured at day 0 are displayed in Table 2. The average value for PCL was around 52 °C for $T_m$. After pretreatment, $T_m$ increased to $c.$ 56.5 °C due to increasing in crystal thickness and perfection indicates higher stability of the crystals.[47] The low temperature melting shoulders were not observed for PCL in the thermophilic samples. This may be attributed to crystal rearrangements occurring at higher temperatures under thermophilic conditions.[40] Untreated PLA at day 0 exhibited $T_g$ and $T_m$ values of around 55.5 °C and 144 °C, respectively. PLA-PT showed a $T_g$ of 60.3 °C and $T_m$ of 148.8 °C. A significant shift toward higher temperatures for the $T_m$ is observed for PCL compared to PCL at day 0, indicating a more ordered and crystalline structure during early stage of biodegradation. However, for PLA, the $T_m$ shows a shift towards lower temperature indicative of the formation of imperfect crystals, especially for PLA-PT samples due to the decrease of $M_\eta$, following the behavior of an adapted Flory–Fox equation reported by Saeidlou *et al.*, 2012 below (4). From the double melting peak displayed can be deducted the formation of $\alpha$-crystal for the highest $T_m$ and $\delta$-crystal form for the lowest $T_m$.[48]

$$T_m = T_m^\infty - \frac{A}{M_\eta} \qquad (4)$$

where $T_m^\infty = 181.3$ °C and $A = 1.02 \times 10^5$ °C g mol$^{-1}$.[48] During crystallization both forms $\alpha$- and $\delta$-crystal are formed with a similar energy and, therefore, able to coexist. From this, the higher $T_m$ corresponds to the more stable $\alpha$ form, while the lower $T_m$ is associated with the less stable $\delta$-crystal.[49] The shift to a lower temperature for $T_m$ of PLA-PT is related to an increase in the crystallinity but indicative of a least ordered crystalline structure probably associated with a $\delta$-structure formation at day 30. The $T_m$ of $\delta$ structure has been reported to be $c.$ 10 °C lower than $\alpha$-crystal, suggesting a less stable $\delta$ form.[48]

### 3.4. Relationship between crystallinity and molecular weight reduction during biodegradation

Abiotic pretreatment may provide advantages over biotic pretreatment by enabling quicker disintegration and increasing the exposed area for microbial attack, while also reducing the $M_\eta$ of the structure and total disintegration of the amorphous region. Additionally, a more resilient $X_c$ typically diminishes abiotic hydrolysis, enzymatic hydrolysis, and the overall biodegradation process. Furthermore, the behavior of surface properties must be considered when enhancing biodegradation performance.

During bulk degradation, when water diffusion into the polymer occurs faster than the hydrolytic attack, the $M_\eta$ decreases early in the process. This decrease in $M_\eta$, along with the increased mobility of shorter polymer segments, the presence of water acting as a plasticizer, and elevated temperatures, can lead to a higher degree of $X_c$.[50] The increase in initial $X_c$ due to the reduction of initial $M_\eta$ is particularly relevant for PLA, but it has minimal effect on PCL due to its larger
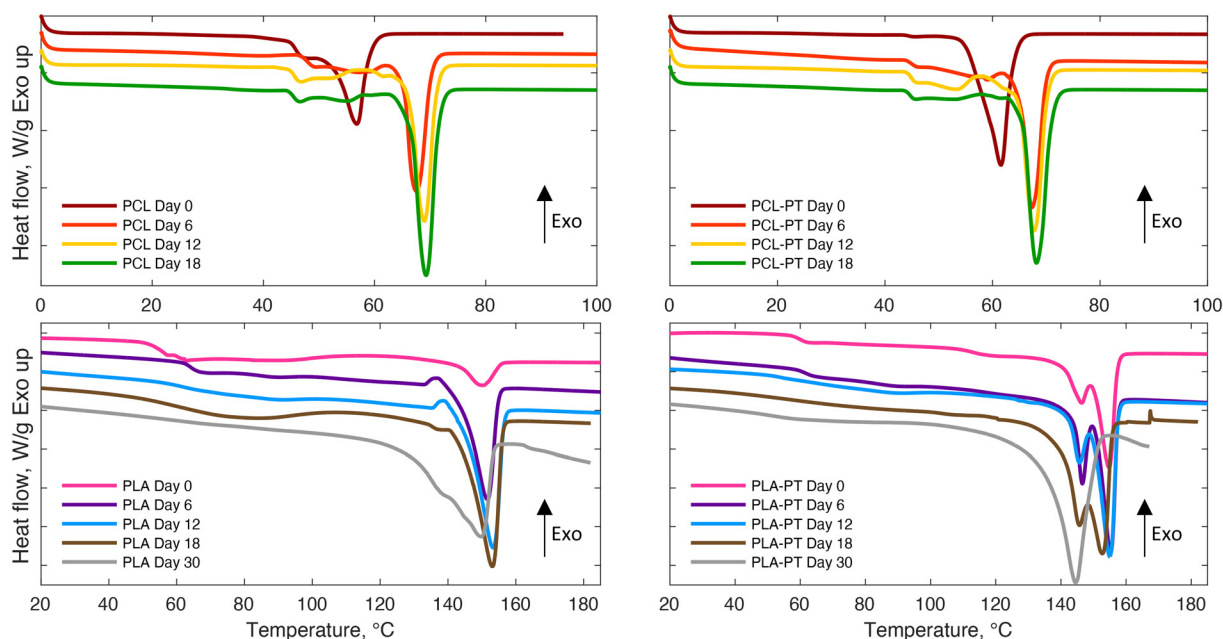


**Fig. 4** Differential scanning calorimetry of PCL (top left), PCL pretreated (top right), PLA (bottom left), and PLA pretreated (bottom right) for day 0 and during the early stage of the biodegradation process.

initial $X_c$. In the case of PLA, the impact of $M_\eta$ reduction on fragmentation and the initiation of depolymerization is more pronounced than for PCL.

For PLA, hydrolysis pretreatment lowers $T_g$ and decreases PLA's $M_\eta$ due to chain scission, enhancing chain mobility and increasing the biodegradation rate. However, the increased $X_c$ formed during hydrolysis can initially slow degradation since crystalline regions are tightly packed and less accessible to water and microorganisms. In contrast, PCL, which starts with a high degree of crystallinity, experiences minimal changes in both $M_\eta$ and $X_c$ after hydrolysis. Consequently, the biodegradation rate of PCL remains relatively unaffected, as its well-formed crystalline structure does not undergo significant changes during hydrolysis.[18]

A common characteristic of hydrolytic degradation processes is that increasing $X_c$ tends to lower the degradation rate. This occurs because water cannot easily penetrate the highly ordered crystalline regions.[39] Although fast crystallization may initially slow biodegradation due to the resistance of crystalline regions, the interaction between crystalline and amorphous regions complicates the prediction. In the rigid amorphous regions (RAFs) formed between the mobile amorphous regions (MAF) and the crystalline domains, the degradation rate could be higher, resulting in an increased biodegradation rate and a more nuanced effect on overall biodegradation,[51] which remains to be decoupled.

## 4. Conclusions

Using hydrolysis as a green and affordable alternative to accelerate biodegradation showed significant improvements for PLA but only modest gains for PCL. This is indicated by the fact that the effect of pretreatment was more pronounced in reducing $M_\eta$ for PLA than for PCL, thus reducing the lag phase of pretreated PLA. When possible, it is essential to ascertain the best optimization strategies for pretreatment, considering the general characteristics of biodegradable polymers, especially polyesters, while also taking into account critical parameters of the media, such as pH for hydrolysis pretreatments at high temperatures. Additionally, altering the surface properties of polymer films through pretreatment can be beneficial, leading to a more effective breakdown process. Understanding the unique attributes of each polymer will facilitate more efficient pretreatments and biodegradation strategies.

## Author contributions

Jordan D'Amario: Experimental run, data collection, writing – original draft, editing, and reviewing, visualization. Anibal Bher: Conceptualization, experimental run, data collection and curation, writing – original draft, editing, and reviewing, supervision, validation. Wanwarang Limsukon: Experimental run, data collection and curation, visualization, writing – original draft, editing, and reviewing. Rafael Auras: conceptualization, writing – original draft, editing and reviewing, funding acquisition, supervision. All the authors approved the final version of the manuscript.

## Data availability

Data is available in the manuscript, and additional raw data supporting this article has been included as part of the ESI.†

## Conflicts of interest

There are no conflicts to declare.

## Acknowledgements

## References

1 The White House, *Bold Goals for U.S. Biotechnology and Biomanufacturing: Harnessing Research and Development to Further Societal Goals*, 2023.

2 UNEP, *Turning off the Tap How the world can end plastic pollution and create a circular economy*, 2023, Available from: https://www.unep.org/resources/turning-off-tap-end-plastic-pollution-create-circular-economy.

3 World Bank, *What a Waste 2.0 A Global Snapshot of Solid Waste Management to 2050 Overview*, 2018.

4 X. E. Crystal Thew, S. C. Lo, R. N. Ramanan, B. T. Tey, N. D. Huy and O. Chien Wei, Enhancing plastic biodegradation process: strategies and opportunities, *Crit. Rev. Biotechnol.*, 2024, **44**(3), 477–494.

5 Closed Loop Partners, *The Realities of Compostable Packaging Disintegration in Composting Systems Breaking it Down*, 2024, Available from: https://www.closedlooppartners.com.

6 Nordic Council of Ministers, Towards Ending Plastic Pollution by 2040, 15 Global Policy Interventions for Systems Change, 2023, Available from: https://www.norden.org.

7 R. C. Thompson, W. Courtene-Jones, J. Boucher, S. Pahl, K. Raubenheimer and A. A. Koelmans, Twenty years of microplastics pollution research—what have we learned?, *Science*, 2024, **386**(6720), eadl2746, Available from: https://www.science.org/doi/10.1126/science.adl2746.

© 2025 The Author(s). Published by the Royal Society of Chemistry

*RSC Appl. Polym.*, 2025, **3**, 711–721 | 719

8  S. Nizamuddin, A. J. Baloch, C. Chen, M. Arif and N. M. Mubarak, Bio-based plastics, biodegradable plastics, and compostable plastics: biodegradation mechanism, biodegradability standards and environmental strategem, *Int. Biodeterior. Biodegrad.*, 2024, **195**, 105887.

9  R. Auras, H. Tsuji, S. Selke and L. Loong-Tak, *Poly(Lactic Acid) synthesis, structures, properties, processing*, Wiley-Blackwell, 2022.

10  L. K. Ncube, A. U. Ude, E. N. Ogunmuyiwa, R. Zulkifli and I. N. Beas, Environmental impact of food packaging materials: A review of contemporary development from conventional plastics to polylactic acid based materials, *Materials*, 2020, **13**, 1–24.

11  C. Sun, S. Wei, H. Tan, Y. Huang and Y. Zhang, Progress in upcycling polylactic acid waste as an alternative carbon source: A review, *Chem. Eng. J.*, 2022, **446**, 136881.

12  G. L. Siparsky, K. J. Voorhees and F. Miao, Hydrolysis of Polylactic Acid (PLA) and Polycaprolactone (PCL) in Aqueous Acetonitrile Solutions: Autocatalysis, *J. Environ. Polym. Degrad.*, 1998, **6**, 31–41.

13  M. A. Woodruff and D. W. Hutmacher, The return of a forgotten polymer - Polycaprolactone in the 21st century, *Prog. Polym. Sci.*, 2010, **35**, 1217–1256.

14  M. Thakur, I. Majid, S. Hussain and V. Nanda, Poly(ε-caprolactone): A potential polymer for biodegradable food packaging applications, *Packag. Technol. Sci.*, 2021, **34**, 449–461.

15  A. Bher, I. U. Unalan, R. Auras, M. Rubino and C. E. Schvezov, Graphene modifies the biodegradation of poly(lactic acid)-thermoplastic cassava starch reactive blend films, *Polym. Degrad. Stab.*, 2019, **164**, 187–197.

16  H. Wan, C. Sun, C. Xu, B. Wang, Y. Chen, Y. Yang, *et al.*, Synergistic reinforcement of polylactic acid/wood fiber composites by cellulase and reactive extrusion, *J. Cleaner Prod.*, 2024, **434**, 140207.

17  S. S. Hamdani, H. M. Elkholy, M. O. Alghaysh, I. Wyman, A. Bher, R. Auras, *et al.*, Recyclable and Biodegradable Paper Coating with Functionalized PLA and PBAT, *ACS Omega*, 2025, **10**(11), 11483–11497.

18  I. Castilla-Cortázar, J. Más-Estellés, J. M. Meseguer-Dueñas, J. L. Escobar Ivirico, B. Marí and A. Vidaurre, Hydrolytic and enzymatic degradation of a poly(ε-caprolactone) network, *Polym. Degrad. Stab.*, 2012, **97**(8), 1241–1248.

19  W. Limsukon, M. Rubino, M. Rabnawaz, L. T. Lim and R. Auras, Hydrolytic degradation of poly(lactic acid): Unraveling correlations between temperature and the three phase structures, *Polym. Degrad. Stab.*, 2023, **217**, 110537.

20  Waste Dive, *Compostable packaging's relationship status with organics recyclers: 'It's complicated'*, 2024, Available from: **https://www.wastedive.com/news/bpi-summit-compostable-packaging-usda-calrecycle/** [cited 2024 Sep 25].

21  E. Gastaldi, F. Buendia, P. Greuet, Z. Benbrahim Bouchou, A. Benihya, G. Cesar, *et al.*, Degradation and environmental assessment of compostable packaging mixed with biowaste in full-scale industrial composting conditions, *Bioresour. Technol.*, 2024, **400**, 130670.

22  A. Bher, Y. Cho and R. Auras, Boosting Degradation of Biodegradable Polymers, *Macromol. Rapid Commun.*, 2023, **44**, e2200769.

23  T. Kijchavengkul, R. Auras, M. Rubino, M. Ngouajio and R. T. Fernandez, Assessment of aliphatic–aromatic copolyester biodegradable mulch films. Part I: Field study, *Chemosphere*, 2008, **71**(5), 942–953.

24  T. Kijchavengkul, R. Auras, M. Rubino, M. Ngouajio and R. T. Fernandez, Assessment of aliphatic–aromatic copolyester biodegradable mulch films. Part II: Laboratory simulated conditions, *Chemosphere*, 2008, **71**(9), 1607–1616.

25  N. Mat Yasin, S. Akkermans and J. F. M. Van Impe, Enhancing the biodegradation of (bio)plastic through pretreatments: A critical review, *Waste Manage.*, 2022, **150**, 1–12.

26  Z. H. W. Easton, M. A. J. Essink, L. Rodriguez Comas, F. R. Wurm and H. Gojzewski, Acceleration of Biodegradation Using Polymer Blends and Composites, *Macromol. Chem. Phys.*, 2023, **224**, 2200421.

27  M. Yusefi, M. Khalid, F. M. Yasin, L. C. Abdullah, M. R. Ketabchi and R. Walvekar, Performance of Cow Dung Reinforced Biodegradable Poly(Lactic Acid) Biocomposites for Structural Applications, *J. Polym. Environ.*, 2018, **26**(2), 474–486.

28  H. Tsuji, Hydrolytic Degradation, in *Poly(Lactic Acid)*, 2022, pp. 467–516, DOI: **10.1002/9781119767480.ch21**.

29  F. Iñiguez-Franco, R. Auras, G. Burgess, D. Holmes, X. Fang, M. Rubino, *et al.*, Concurrent solvent induced crystallization and hydrolytic degradation of PLA by water-ethanol solutions, *Polymer*, 2016, **99**, 315–323.

30  J. R. Dorgan, J. Janzen, D. M. Knauss, S. B. Hait, B. R. Limoges and M. H. Hutchinson, Fundamental solution and single–chain properties of polylactides, *J. Polym. Sci., Part B:Polym. Phys.*, 2005, **43**(21), 3100–3111.

31  H. Sun, L. Mei, C. Song, X. Cui and P. Wang, The in vivo degradation, absorption and excretion of PCL-based implant, *Biomaterials*, 2006, **27**(9), 1735–1740.

32  H. L. Chen, L. J. Li and T. L. Lin, Formation of Segregation Morphology in Crystalline/Amorphous Polymer Blends: Molecular Weight Effect, *Macromolecules*, 1998, **31**(7), 2255–2264, Available from: **https://pubs.acs.org/sharingguidelines**.

33  E. W. Fischer, H. J. Sterzel and G. Wegner, Investigation of the structure of solution grown crystals of lactide copolymers by means of chemical reactions, *Z-Polymers*, 1973, **251**, 980–990.

34  E. Castro-Aguirre, R. Auras, S. Selke, M. Rubino and T. Marsh, Insights on the aerobic biodegradation of polymers by analysis of evolved carbon dioxide in simulated composting conditions, *Polym. Degrad. Stab.*, 2017, **137**, 251–271, Available from: **https://linkinghub.elsevier.com/retrieve/pii/S0141391017300241**.

35  T. Kijchavengkul, R. Auras, M. Rubino, M. Ngouajio and R. Thomas Fernandez, Development of an automatic laboratory-scale respirometric system to measure polymer biodegradability, *Polym. Test.*, 2006, **25**(8), 1006–1016.

36 A. Leroux, T. Ngoc Nguyen, A. Rangel, I. Cacciapuoti, D. Duprez, D. G. Castner, *et al.*, Long-term hydrolytic degradation study of polycaprolactone films and fibers grafted with poly(sodium styrene sulfonate): Mechanism study and cell response, *Biointerphases*, 2020, **15**(6), 061006.

37 G. G. Pitt, M. M. Gratzl, G. L. Kimmel, J. Surles and A. Sohindler, Aliphatic polyesters II. The degradation of poly (DL-lactide), poly (ε-caprolactone), and their copolymers in vivo, *Biomaterials*, 1981, **2**(4), 215–220.

38 H. Tsuji, T. Ishida and N. Fukuda, Surface hydrophilicity and enzymatic hydrolyzability of biodegradable polyesters: 1. effects of alkaline treatment, *Polym. Int.*, 2003, **52**(5), 843–852.

39 B. Laycock, M. Nikolić, J. M. Colwell, E. Gauthier, P. Halley, S. Bottle, *et al.*, Lifetime prediction of biodegradable polymers, *Prog. Polym. Sci.*, 2017, **71**, 144–189.

40 C. Eldsäter, The biodegradation of amorphous and crystalline regions in film-blown poly(ε-caprolactone), *Polymer*, 2000, **41**(4), 1297–1304.

41 H. Tsuji and K. Suzuyoshi, Environmental degradation of biodegradable polyesters 1. Poly(ε-caprolactone), poly[(R)-3-hydroxybutyrate], and poly(L-lactide) films in controlled static seawater, *Polym. Degrad. Stab.*, 2002, **75**(2), 347–355.

42 A. Göpferich, Mechanisms of polymer degradation and erosion, *Biomaterials*, 1996, **17**(2), 103–114.

43 F. von Burkersroda, L. Schedl and A. Göpferich, Why degradable polymers undergo surface erosion or bulk erosion, *Biomaterials*, 2002, **23**(21), 4221–4231.

44 A. Fernández-Tena, R. A. Pérez-Camargo, O. Coulembier, L. Sangroniz, N. Aranburu, G. Guerrica-Echevarria, *et al.*, Effect of Molecular Weight on the Crystallization and Melt Memory of Poly(ε-caprolactone) (PCL), *Macromolecules*, 2023, **56**(12), 4602–4620.

45 E. Castro-Aguirre, F. Iñiguez-Franco, H. Samsudin, X. Fang and R. Auras, Poly(lactic acid)—Mass production, processing, industrial applications, and end of life, *Adv. Drug Delivery Rev.*, 2016, **107**, 333–366.

46 A. Larrañaga and E. Lizundia, A review on the thermomechanical properties and biodegradation behaviour of polyesters, *Eur. Polym. J.*, 2019, **121**, 109296.

47 A. Wurm, E. Zhuravlev, K. Eckstein, D. Jehnichen, D. Pospiech, R. Androsch, *et al.*, Crystallization and homogeneous nucleation kinetics of poly(ε-caprolactone) (PCL) with different molar masses, *Macromolecules*, 2012, **45**(9), 3816–3828.

48 S. Saeidlou, M. A. Huneault, H. Li and C. B. Park, Poly (lactic acid) crystallization, *Prog. Polym. Sci.*, 2012, **37**(12), 1657–1677.

49 M. Yasuniwa, S. Tsubakihara, K. Iura, Y. Ono, Y. Dan and K. Takahashi, Crystallization behavior of poly(l-lactic acid), *Polymer*, 2006, **47**(21), 7554–7563.

50 W. Limsukon, R. Auras and S. Selke, Hydrolytic degradation and lifetime prediction of poly(lactic acid) modified with a multifunctional epoxy-based chain extender, *Polym. Test.*, 2019, **80**, 106108.

51 X. Han and J. Pan, A model for simultaneous crystallisation and biodegradation of biodegradable polymers, *Biomaterials*, 2009, **30**(3), 423–430, Available from: **https://linkinghub.elsevier.com/retrieve/pii/S0142961208007424**.

© 2025 The Author(s). Published by the Royal Society of Chemistry

*RSC Appl. Polym.*, 2025, **3**, 711–721 | **721**